Volume conductor effects on the spatial resolution of magnetic fields and electric potentials from gastrointestinal electrical activity

L. A. Bradshaw[1,2,3] W. 0. Richards[2,4] J. P. Wikswo Jr'

'Living State Physics Group, Department of Physics &Astronomy, Vanderbilt University, Nashville, Tennessee, USA
'Department of Surgery, Vanderbilt University Medical Center, Nashville, Tennessee, USA
[3]Lipscomb University, Nashville, Tennessee, USA
[4]Department of Surgery, Veterans' Affairs Medical Center, Nashville, Tennessee, USA

Abstract-An ***analysis of the relative capabilities of methods for magnetic and electric detection of gastrointestinal electrical activity is presented. The model employed is the first volume conductor model for magnetic fields from GEA to appear in the literature. A mathematical model is introduced for the electric potential and magnetic field from intestinal electrical activity in terms of the spatial filters that relate the bioelectric sources with the external magnetic fields and potentials. The forward spatial filters are low-pass functions of spatial frequency, so more superficial external fields and potentials contain less spatial information than fields and potentials near the source. Inverse spatial filters, which are reciprocals of the forward filters, are high-pass functions and must be regularised by windowing. Because of the conductivity discontinuities introduced by low-conductivity fat layers in the abdomen, the electric potentials recorded outside these layers required more regularisation than the magnetic fields, and thus, the spatial resolution of the magnetic fields from intestinal electrical activity is higher than the spatial resolution of the external potentials. In this study, two smooth muscle sources separated by 5cm were adequately resolved magnetically, but not resolved electrically. Thus, sources are more accurately localized and imaged using magnetic measurements than using measurements of electric potential.***

Keywords-Magnetogastrogram, Electrogastrogram, Smooth muscle electrical activity

Med. Biol. Eng. Comput., 2001,39,35-43

1 Introduction

SMOOTH MUSCLE of the gastrointestinal (GI) system controls the complex processes of digestion. The electrical control activity (ECA) is a slow oscillation in the resting membrane potential that is always present. The electrical response activity (ERA) consists of a plateau phase and a higher frequency spiking phase that occurs when the ECA has sufficiently depolarised the membrane (DANIEL *et* al., 1959).

Gastrointestinal smooth muscle behaves as an electrical syncytium (DANIEL and SARNA, 1978), i.e., all cells behave as though electrically interconnected by gap junctions. In the stomach, gastric electrical activity originates at a pacemaker located in the corpus and propagates aborally towards the pylorus. GEA frequency throughout the gastric musculature is about 3 cycles min^{-1}. In the small intestine, electrical activity is propagated from several pacemaker locations, and exhibits a gradient in frequency from 12 cycles min^{-1} in the duodenum to 8 cycles min^{-1} in the terminal ileum (FLECKENSTEIN, 1978).

Correspondence should be addressed to Dr L. A. Bradshaw; email: /eonard.a.bradshaw@vanderbi/t.edu

First received IO January 2000 and in final form 7 November 2000
MBEC online number: 20013539

Fig. 1 illustrates how the electric currents and potentials associated with the movement of ions across smooth muscle membranes produce both extracellular electric potentials and magnetic fields. The electrogastrogram (EGG) records electric potentials from gastric electrical activity with cutaneous electrodes placed on the abdominal surface. However, of the parameters that describe GEA (amplitude, frequency, phase, propagation velocity), frequency dynamics of the EGG signal has been the only reliable parameter (MINTCHEV *et al.*, 1993). The electroenterogram (EENG), the recording of cutaneous potentials from intestinal electrical activity, cannot be reliably obtained at the abdominal surface unless intervening abdominal layers are removed (CHEN *et al.*, 1993*a*; SMOUT *et al.*, 1984).

The magnetogastrogram (MGG) and magnetoenterogram (MENG) record the magnetic fields from gastric and intestinal electrical activity, respectively. In contrast to electric potentials, magnetic fields of both the stomach and small bowel are always recordable (*RICHARDS et* al., 1996). Previous studies have demonstrated that the MGG and MENG correlate well with internal serosal activity (BRADSHAW *et al.*, 1997), and allow identification of the ECA frequency gradient (Richards *et al.*, 1996) as well as the characteristics of ECA propagation (BRADSHAW *et* al., 1999a).

Disease states in the stomach and small bowel are known to change parameters of the electrical activity of smooth muscle (TELANDER *et al.*, 1978; KOCH *et al.*, 1989,199O; DEVANE *et al.*,

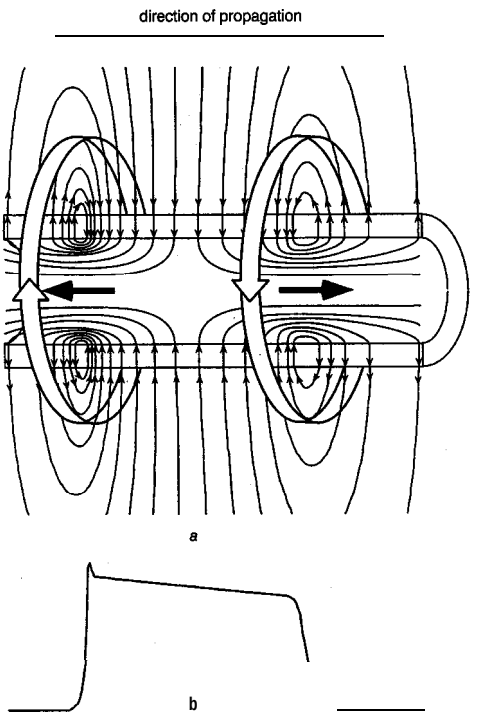

*Fig. 1 Movement of ions across the membmne of smooth muscle cells associated with changes in membmne potential creates intracellular **current flow** along the cell, creating both **extracellular potentials** and **magnetic fields***

1992; **HONKO** and **OKUNO, 1993; ROTHSTEIN** *et* **al., 1993; HASLER et al.,** 1995; **DEBINSKI** *et* al., 1996). Bradygastria, tachygastria, and cell uncoupling have been observed in cutaneous electrode studies of gastric disease states such as gastroparesis **(ABELL** ***et al.,*** **1985; ABELL** and **MALAGELADA** *et al.,* **1985; PFISTER** *et al.,* 1988; FAMILONI *et al.,* 1991; *CHEN* and **MCCALLUM,** 1992; *CHEN et* al., 1993b), although no conclusive studies validating the existence of bradygastria and tachygastria with internal recordings have appeared **(MINTCHEV** and **BOWES,** 1997; MINTCHEV *et* al., 1997). Changes in propagation of electrical activity during disease or mechanical uncoupling have also been measured using internal electrodes **(BEDI et al.,** 1972; *YOU et* al., 1980). Thus, the ability to noninvasively measure gastric and intestinal electrical activity has important clinical implications.

Cutaneous electrodes often do not reflect the changes in gastrointestinal electrical activity that occur during the disease state **(MINTCHEV** and **BOWES,** 1997; MINTCHEV *et* al., 1997). Several authors have suggested that spatial smearing caused by low conductivity abdominal layers is responsible for the lack of spatial detail in the external potentials. Previous research *(BRADSHAW et al.,* 1999b) has shown that magnetic fields are not as affected by low conductivity layers as electric potentials, so non-invasive detection of magnetic fields from GI activity may provide information not available in cutaneous recordings of electric potentials. Both model simulations and experimental results show that the magnetoencephalogram, for instance, provides greater spatial resolution than the electroencephalogram. It was previously shown that the low conductivity of the skull, in conjunction with the higher conductivity cortex and scalp, reduces both the localising and imaging resolution of the EEG (BRADSHAW *et al.,* 1999b).

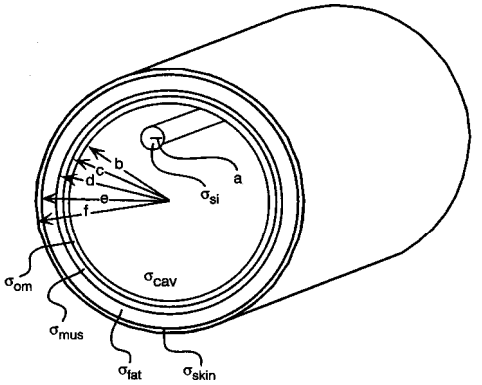

Fig. 2 *The abdomen is represented by a concentric cylinders model **with five** layers that represent the abdominal **cavity, omentum,** abdominal muscle, subcutaneous fat. and skin. Sources of **electrical activity** are contained in the small intestine, **an** eccentric cylinder of radius a located in the abdominal cavity*

To examine the magnetic fields and electric potentials from gastrointestinal electrical activity, we present a volume conductor model with five concentric cylindrical layers. The model is employed to examine the effects ofabdominal layers on the external signals and uses the concept of spatial filters, which describe the analytical relationship between the internal electrical sources and the external fields and potentials. The spatial filter construct allows one to graphically visualize the effects of the layers on the spatial resolution of the external signals.

Although the model may be applied to both gastric and intestinal signals, we concentrate on analysis of the electroenterogram (EENG) and magnetoenterogram (MENG). This is the first mathematical model describing the magnetic fields from gastrointestinal electrical activity.

2 Methods

2.1 The abdominal model

The abdominal cavity is modelled as a cylinder of **infinite** length aligned along the z-axis as shown in Fig. 2, with layers representing omentum, muscle, subcutaneous fat, and skin. The small intestine, represented by an eccentric cylinder in the abdominal cavity of radius a, is the source of electrical activity. Model parameters and the nominal values used in this analysis are shown in Table 1.

The source of electrical activity in this model is the membrane potential of the smooth muscle of the intestine. The slow wave consists of an initial depolarisation followed by a prolonged

Table 1 Typical abdominal model parameter values"

Parameter	Value	Parameter	Value	Parameter	Value
a	8.0 mm	$\|r'\|$	6.5 cm	σ_{skin}	0.45/R In
b	7.8 cm	R	Varies	θ_a	Varies
c	8.3 cm	σ_{si}	0.88/Ω·m	t_{om}	5.0 mm
d	8.8 cm	σ_{cav}	0.45/Ω m	t_{mus}	5.0 mm
e	10.0 cm	σ_{om}	0.02/Ω· m	t_{fat}	12.0 mm
f	10.5 cm	σ_{mus}	0.45/Ω m	t_{skin}	5.0 mm
$\|r\|$	Varies	σ_{fat}	0.02/Ω m		

"Conductivity values are taken from SCHWAN, H. P., and KAY, C. F. The conductivity of living tissues. *Annals of NY Acad. Sci. 65, pp.* 1007-1013, 1957. Geometrical parameters are taken from SNELL, R. M. *Clinical Anatomy for Medical Students.* Little, Brown & Co., Boston, 1986.

plateau potential and gradual repolarisation. For simplicity, the slow wave is represented by a Gaussian waveform defined by its amplitude (10 mV), width (1 cm), and location along the z-axis. To investigate the differences in spatial properties of electric potentials and magnetic fields, we use two slow waves separated by 5 cm. The membrane potential and the intracellular current associated with it are shown in Fig. 3.

Electric potentials and magnetic fields may be calculated at any location in or outside the volume conducting medium. Furthermore, the magnetic field is a vector quantity, and we can calculate both radial (r) and tangential (θ) components of the vector magnetic field. The z-component of the magnetic field in this model is identically zero, since the intracellular current sources associated with the membrane potential are aligned with the z-axis.

2.2 Spatial filter relationships

The external electric potential and magnetic field are calculated from the internal membrane potential or intracellular current density of smooth muscle cells. If the extracellular conductivity is sufficiently high (core-conductor limit), the intracellular current density is related to the membrane potential by (WOOSLEY *et al.*, 1985)

$$\boldsymbol{J}^i(\boldsymbol{r}') = \sigma_i \nabla \Phi_m(\boldsymbol{r}') \tag{1}$$

where $\boldsymbol{r}'$ is a vector to the source location, $\boldsymbol{J}(\boldsymbol{r}')$ is the intracellular current density, σ_i is the conductivity of the smooth muscle, and $\Phi_m(\boldsymbol{r}')$ is the membrane potential. If the membrane potential varies only along z, then the Fourier transform of eqn 1 is

$$j^i(k_z) = \sigma_i k \phi_m(k_z) \tag{2}$$

where k is the spatial frequency, and lower-case quantities correspond to frequency domain representations of the upper-case quantities. The factor $\sigma_i k$ can be thought of as a spatial filter that, when applied to the spatial frequency domain representation of the membrane potential, gives the intracellular current density. Thus, this spatial filter represents the relationship between the membrane potential and the intracellular current density. It is closely related to the concept of transfer functions.

We can also specify the relationships between the source and the measured electric potential or magnetic fields in terms of spatial filters, which are essentially the Green's functions of the forward equations for the potential and magnetic field:

$$\Phi(\boldsymbol{r}) = \frac{1}{4\pi\sigma}\int_{\Omega} \frac{\nabla \cdot \boldsymbol{J}(\boldsymbol{r}')}{|\boldsymbol{r}-\boldsymbol{r}'|} d\boldsymbol{r}' \tag{3}$$

and

$$\mathrm{B}(\mathrm{r}) = \frac{\mu}{4\pi}\int_{\Omega} \frac{\nabla \times \boldsymbol{J}(\boldsymbol{r}')}{|\boldsymbol{r}-\boldsymbol{r}'|} d\boldsymbol{r}' \tag{4}$$

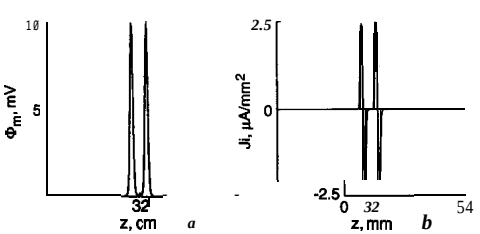

Fig. 3 (a) The smooth muscle transmembrane potential is the source of electrical activity in this model. (b) The intracellular current associated with the membrane potential in (a) could also be considered the source of electrical activity

where σ and μ are the conductivity and magnetic permeability of the intracellular medium. The integrations in eqns 3 and 4 extend over the source region, Ω. If the source varies alongz, the Fourier transforms of eqns 3 and 4 are

$$\phi(r, \theta, k_z) = g_{j\phi}(r, r', \theta, k_z) j^i(r', \theta, k_z) \tag{5}$$

$$b(r, \theta, k_z) = g_{jb}(r, r', \theta, k_z) j^i(r', \theta, k_z) \tag{6}$$

where θ describes the polar angle of the cylindrical model. The forward spatial filters $g_{j\phi}$ and g_{jb} are defined by the Fourier transform of the integration kernel, as described elsewhere (BRADSHAW, 1995). The membrane potential may be used as the source function in place of the intracellular current density

$$\phi(r, \theta, k_z) = g_{\phi_m\phi}(r, r', \theta, k_z) \phi_m(r', \theta, k_z) \tag{7}$$

$$b(r, \theta, k_z) = g_{\phi_m b}(r, r', \theta, k_z) \phi_m(r', \theta, k_z) \tag{8}$$

The forward spatial filters are dependent on the passive geometrical and electrical properties of the volume conducting abdomen and describe the relationship between the internal source and extracellular potentials and magnetic fields.

We would like to be able to solve the inverse problem of determining the internal sources from external measurements of electric potential and magnetic field. Within the spatial filter framework, the inverse problem is solved by rearranging eqns 7 and8

$$\phi_m(r, \theta, k_z) = \frac{1}{g_{\phi_m\phi}(r, \theta, k_z)} \phi(r, \theta, k_z) \tag{9}$$

$$\phi_m(r, \theta, k_z) = \frac{1}{g_{\phi_m b}(r, \theta, k_z)} b(r, \theta, k_z) \tag{10}$$

Thus, the inverse spatial filters are simply reciprocals of the forward spatial filters

$$g_{\phi\phi_m}(r, \theta, k_z) = \frac{1}{g_{\phi_m\phi}(r, \theta, k_z)} \tag{11}$$

$$g_{b\phi_m}(r, \theta, k_z) = \frac{1}{g_{\phi_m b}(r, \theta, k_z)} \tag{12}$$

In general, the inverse problem is ill-posed in that it is non-unique (different configurations of sources may produce the same external potentials or magnetic fields) and poorly conditioned (inverse solutions are unstable in the presence of noise) (PARKER, 1977). The spatial filter analysis we present avoids the non-uniqueness issue by restricting the solution space to particular values of r and θ; we allow the source to vary only along the z-direction.

2.3 Evaluation of spatial resolution

In this work, we apply the spatial filter construct to investigate the spatial resolution available in the EENG and the MENG. The approach to the problem is illustrated in Fig. 4. The forward problem is calculated using the forward spatial filters, which are generally low-pass functions of spatial frequency (Fig. 4*c*); the forward fields and potentials contain less spatial information than the internal sources. Simulated, uniform, white measurement noise is then added to the raw signals at a level of 1% with respect to the signal levels at the surface of the abdominal cavity (Fig. 4*f*) and the noisy signal is inverse transformed (Fig. 4g). Since the forward filters are low-pass functions of spatial frequency, the inverse filters are high-pass in nature. Thus, the measurement noise, present equally at all spatial frequencies, is preferentially amplified in the higher spatial frequencies by the inverse filter. This amplification illustrates the ill-conditioned

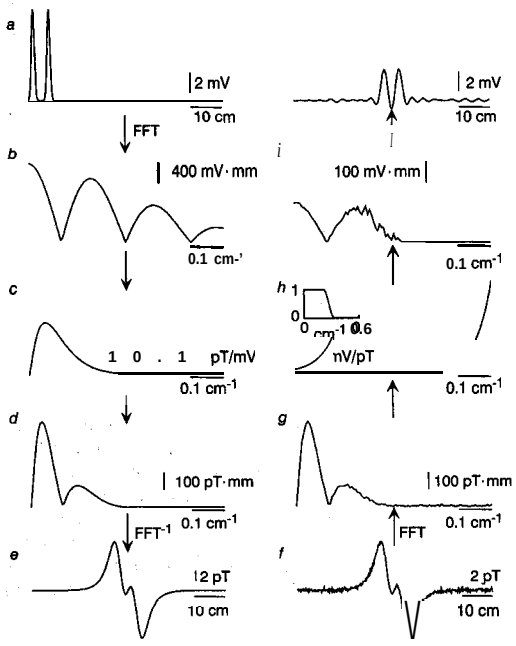

Fig. 4 *The real-space transmembmne potential (a) is Fourier transformed (b) and multiplied with the forward spatial filter (c) to obtain the Fourier transform of the magnetic field (d). The tangential magnetic field and electric potential may be calculated similarly. The real-space radial MENG (e) is obtained by inverse Fourier transformation. To investigate spatial resolution, we add simulated measurement noise to the MENG signal (f) and then multiply its frequency-space representation (g) by the inverse spatialjilter (h), regularised by windowing with a Tukey window with an appropriate cutoff frequency (inset of h), to obtain the Fourier transform of the reconstructed source membrane potential (i), which is then inverse transformed to yield the real-space reconstructed membrane potential (j)*

nature of the inverse problem in that small instabilities in the raw EENG or MENG signals are amplified by the inverse procedure and can result in unstable inverse solutions. The inverse filter must thus be regularised, which is accomplished using a Tukey window (inset of Fig. 4h). The window presents noise in the high spatial frequencies from dominating the reconstructed sources. However, because of the windowing, the reconstructed membrane potential contains less spatial detail than the original membrane potential (Fig. 4*j*). Thus, the effect of regularising the inverse solution is to stabilise the source reconstruction at the expense of spatial resolution.

To evaluate the EENG and MENG on an equal footing, we require that source reconstructions attain a pre-set stability. We restrict ourselves to considerations of stable source solutions, defined by the ratio of the variance in a reconstruction without noise added to the variance in the reconstruction from noisy data:

$$\xi = \frac{\sigma^2_{\Phi_{\text{rec,noiseless}}}}{\sigma^2_{\Phi_{\text{rec,noisy}}}} \qquad (13)$$

We also used this parameter in earlier work on the EEG and MEG (BRADSHAW et al., 1999b). The stability parameter varies from a value of 0, which indicates a completely unstable solution, to a value of 1, which indicates a perfect source reconstruction. We require our inverse solutions to attain a stability of at least 0.98, a value we determined empirically.

By reconstructing sources under these conditions, we can examine the characteristics of both the forward and inverse problems and observe the effects of the volume conducting medium on spatial resolution. Specifically, we investigate how the abdomen attenuates and smooths electric potentials and magnetic fields, study the effect of regularising the inversion, and compare characteristics of the reconstructed source with the original membrane potential. Both the localizing resolution, which measures how accurately a particular source is located, and the imaging resolution, which measures how closely the reconstructed source resembles the original source, are evaluated. The localizing resolution is evaluated by simply comparing the location of the peaks in the Gaussian waveforms. Imaging resolution is evaluated by the Rayleigh criterion used in optics, which states that the degree of resolution of two sources is given by the ratio of the waveform peaks and valleys. Two sources are considered unresolved if their valley-to-peak ratio is less than 0.81 (BORN and WOLF, 1975).

3 Results

3.1 Forward solutions

The forward spatial filters at five different values of *r are.* displayed in Fig. 5. It can be seen that the forward spatial filters are low-pass functions of spatial frequency; fields and potentials more distant from the source contain less spatial detail as the higher spatial frequencies are attenuated by the forward spatial filters. It is interesting to note that EENG spatial filters fall off at lower spatial frequencies than radial or tangential MENG filters. The 3 dB values of the filters are listed in Table 2. These spatial filters, applied to the frequency domain representation of the membrane potential (Fig. 3a), give us the Fourier transforms of the forward radial and tangential MENGs and the EENGs which may then be inverse transformed to yield their real-space versions (Fig. 6).

Fig. 6 shows that the magnetic field waveforms are similar to the intracellular current density (Fig. 3b) and exhibit four phases, while the waveforms of the electric potentials are similar to the

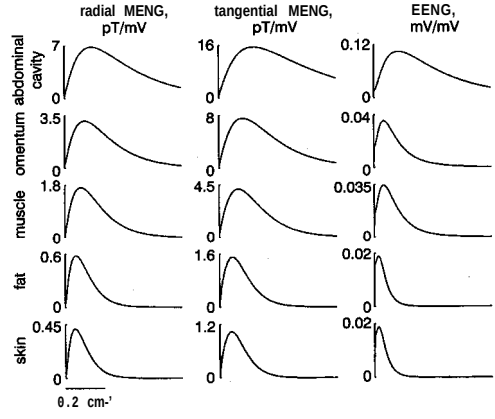

Fig. 5 Forward spatial filters at the surfaces of the five layers of the cylindrical model are lowpass functions of spatial frequency. The spatial filters at mow superficial locationsfall off at lower spatial frequencies, indicating that external fields and potentials at these locations contain less spatial detail. Notice that the forward filters of the electric potential fall off at lower spatial frequencies than those of magnetic fields in the same layer

Table 2 3dB values of forward and inverse spartial filters

	Radial MENG	Tangential MENG	EENG
Abdominal cavity	0.0391	0.0516	0.0378
Omentum	0.0275	0.032	0.0137
Abdominal muscle	0.0214	0.0249	0.0128
subcutaneous fat	0.0140	0.0162	0.0061
Skin	0.0125	0.0143	0.0061

membrane potential (Fig. 3*a*) and exhibit two phases. The signals are clearly smoothed and attenuated with distance from the source, as the amplitudes become smaller and the phases become less distinct. The effect of the low conductivity layers on the EENG is also apparent as the two sources are clearly distinct at the surface of the abdominal cavity, but appear as one source at the cutaneous skin surface.

3.2 Inverse analysis

The inverse spatial filters are plotted in Fig. 7. The MENG signals at the surface of the subcutaneous fat and skin layers, as well as all EENG signals except at the abdominal cavity surface, must be regularised to keep noise from destablising the inversion. The windowed inverse filters under the requirement that the source reconstruction stability be at least 0.98 are also shown. The EENG inverse filters must be regularised at lower frequencies than the corresponding MENG inverse filters. Since the 3 dB points of the EENG filters occur at lower frequencies, white noise is preferentially amplified and destabilises the inversion. In contrast, higher spatial frequencies are admitted into MENG inverse solutions since they are not regularized at such low spatial frequencies.

The source reconstructions obtained from the windowed inverse filters are shown in Fig. 8. These source reconstructions directly reflect the attenuation and smoothing by the layers of the abdominal volume conductor. Whereas the reconstructions from magnetic signals accurately depict two distinct sources at all model layers, reconstructions from the electric potentials appear as one source at the subcutaneous fat and skin layers. It is interesting to note that whereas the magnetic signals steadily degrade at more superficial layers, the reconstructions from the omentnm and abdominal muscle EENG are not substantially different, nor are those from the subcutaneous fat and skin EENGs. Thus, it would appear that the conductivity differences between layers significantly affects the electric potential, but has negligible effects on the magnetic fields.

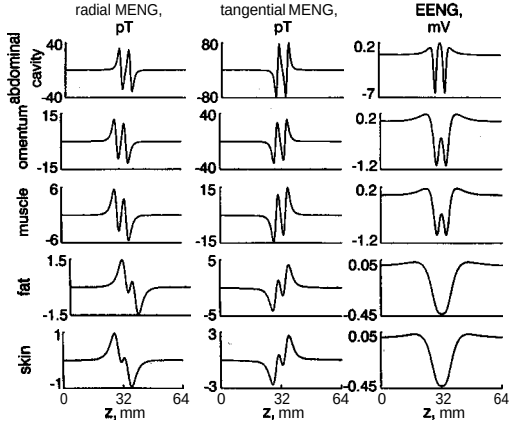

Fig. 6 Radial and tangential MENGs and EENGs at the five interfaces in the abdominal model

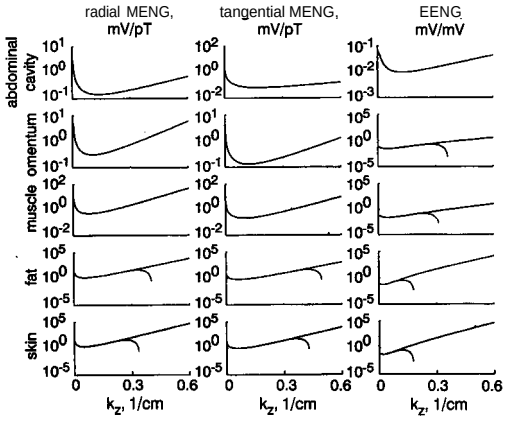

Fig. *7 Inverse spatial jilters are highpass functions of spatial frequency and must be regularised. Windowed inverse filters, determined under the requirement that inverse reconstructions attain a minimum stability (x > 0.98), are also plotted. For the MENG signals through the abdominal muscle layer and the EENG at the surface of the abdominal cavity, the noise level is sufficiently low that no regularisation is required*

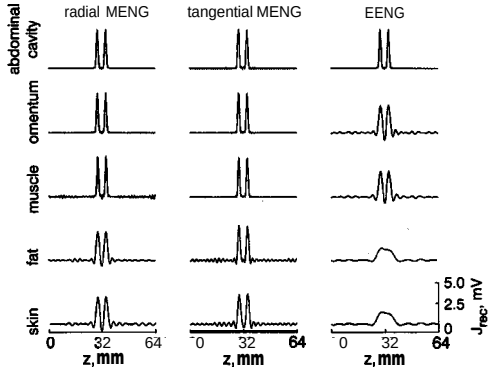

Fig. *8 Source reconstructions under the requirement that the stability be greater than 0.98 accurately reflect thepresence of two distinct sources in the radial and tangential MENG signals, but obscure the sources in the EENG signals at the subcutaneous fat layer and the skin surface*

3.3 Spatial information in EENG and MENG

There are several ways to quantify the amount of spatial information contained in EENG and MENG signals. We first look at the signal amplitudes, starting with calculations at the abdominal cavity/omentum interface and progressing outwards towards the skin surface, to see how the layers of the abdomen affect the raw signals. The amount of spatial information available to any inverse reconstruction depends on the range of spatial frequencies admitted to the inversion. The stability of inverse solutions is controlled by the window cutoff frequency, and it is instructive to examine the relationship between window cutoff frequency and the stability of inverse reconstructions from each of the different methods. We require that the stability of our inverse solutions meet the condition $\xi > 0.98$, which is controlled by decreasing the cutoff frequency of the regularisation window. Thus, we look at how the maximum window cutoff

frequency allows for stable reconstruction changes as a function of distance from the source. Finally, we determine the localising and imaging resolution of stable source reconstructions from EENG and MENG signals through the abdomen.

3.3.1 *Signal amplitude:* The amplitude (peak-to-peak) of the EENG and MENG signals calculated at 1 mm increments through the abdominal layers starting at the inner surface of the omentum to the outer skin surface is plotted in Fig. 9. Both the EENG and MENG decrease in amplitude with distance from the source. However, the EENG exhibits additional attenuation by the low conductivity layers of omentum and subcutaneous fat. While this plot shows the attenuation of the EENG and MENG signals by the abdomen, it does not show the smoothing effects that volume conduction has on the spatial information in the signals. The two distinct sources are smoothed into only one apparent source by the EENG, and thus, the amplitude in the superficial layers near the skin appears stronger than if only one source was present.

3.3.2 Regularization and stability of the inverse solution: To compare the amount of spatial information present in EENG and MENG signals, we examine the resolution of source reconstructions from these signals. Sources are reconstructed from the forward fields and potentials with noise added by applying the inverse spatial filters. These inverse filters are high-pass and must be regularised by windowing. By setting the cutoff frequency of the regularization window, k_{max}, sufficiently low, the amplification of high spatial frequency noise can be reduced and the solution can be made stable. However, the regularisation process reduces the spatial information present in the signals and thus, source reconstructions have less spatial detail. Fig. 10 shows the stability of source reconstructions as the window cutoff frequency is increased. Both MENG and EENG source reconstructions have a stability near 1 for low values of k_{max} and decrease in stability as higher spatial frequencies are admitted to the inversion since noise is amplified by the inverse spatial filters. Source reconstructions from both radial and tangential MENG at the three innermost model interfaces are stable at nearly all

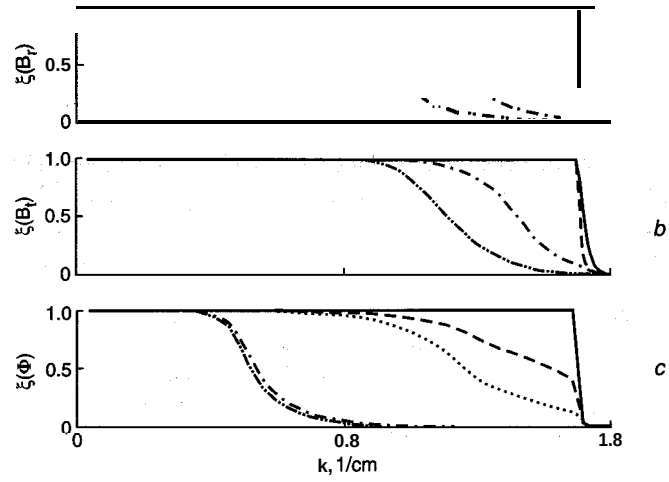

Fig. 10 The stability of source reconstructions from (a) radial MEG, (b) tangential MEG, and (c) EENG as the window cutoff frequency is increased. general, stability decreases as higher spatial frequencies are allowed in the inversion (spatial resolution increases). EENG soucre reconstructions are less stable than MENG source reconstructions at similar window cutoff frequencies. (-) abdominal cavity; (- – -) omentum; (· · ·) muscle; (- · -) fat: (- . . -) skin.

window cutoff frequencies plotted, while the stability of reconstructions from MENG at the surfaces of the subcutaneous fat and skin layers is reduced in spatial frequencies above 0.8 cm-‘. The stability of EENG reconstructions from more superficial layers decrease more quickly as higher spatial frequencies are admitted into the reconstruction. The stability of the subcutaneous fat and skin EENG source reconstructions greatly decreases at window cutoff frequencies above 0.4 cm-‘. Thus, more regularisation is required to keep EENG inverse solutions stable than for MENG reconstructions. The effect of increased regularisation is not only increased stability, but also decreased spatial resolution.

In fact, the maximum window cutoff frequency allowed in an inversion with a stability restricted to a value greater than 0.98 is a measure of the spatial information in the signal. The amount of regularisation required for stable solutions ($\xi > 0.98$) from

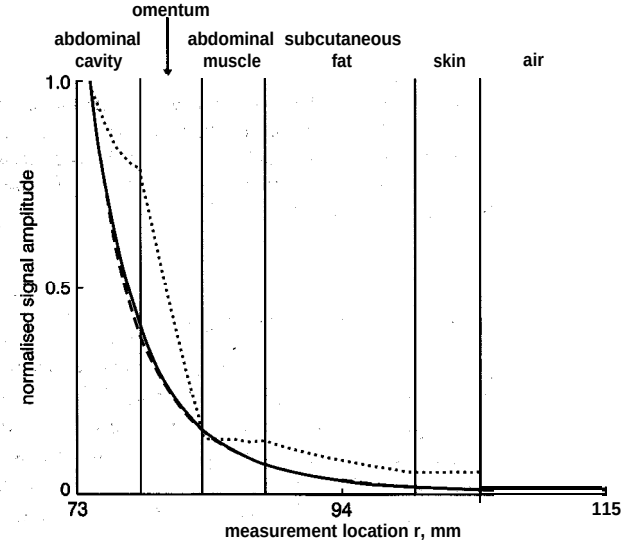

Fig. 9 *The peak-to-peak amplitude of EENG and radial and tangential MENG signals normalized to their values at the abdominal cavity1 omentun interface as a junction of measurement location. The source is located at a radial distance of r = 65 mm. The amplitude of radial and tangential MENG decreases as a junction of distance from the source, but the EENG amplitude is also affected by the low-conductivity omentum and subcutaneous fat layers. (-) radial MENG; (- – -) tangential MENG; (· · ·) EENG.*

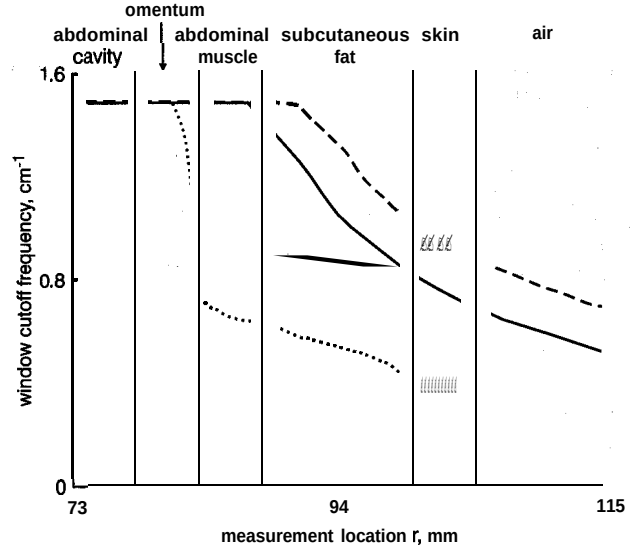

Fig. 11 The maximum window cutoff frequency required for stable solutions from EENG and MENG signals decreases as measurements become more superficial. The omentum and subcutaneous fat layers significantly decrease the maximum window cutoff frequency allowed and consequently, decrease the spatial resolution of source reconstructions from the EENG. (-) radial MENG; (- – -) tangential MENG; (· · ·) EENG.

EENG and MENG signals throughout the abdominal model is plotted in Fig. 11. The tangential MENG requires the least amount of regularisation for a given measurement position, while the EENG requires the most regularisation. The EENG is significantly affected by the presence of the low conductivity omentum and subcutaneous fat layers, while the magnetic fields appear to be insensitive to the presence of these layers.

3.3.3 Source localisation and imaging resolution: The location of sources reconstructed from EENG and MENG signals at the different model layers is shown in Fig. 12. Sources are located correctly for all modalities measured through the subcutaneous fat layer, but sources reconstructed from the EENG outside that layer are localised to one location midway between the correct positions. The MENG correctly localises the sources at all measurement locations.

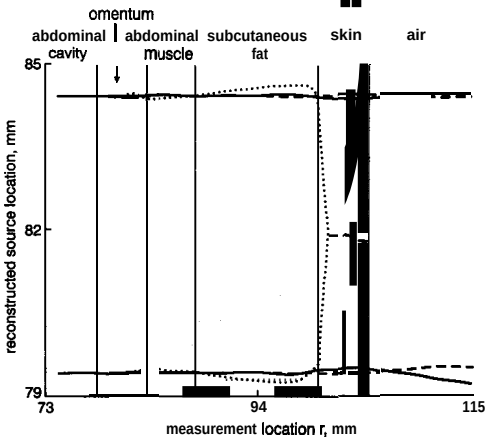

Fig. **12** *The localizing resolution of the reconstructed sources from EENG and MENG is sufficient to resolve the two sources at all locations except for those the EENG outside the subcutaneous fat layer. (——) radial MENG; (- – -) tangential MENG; (· ·) EENG.*

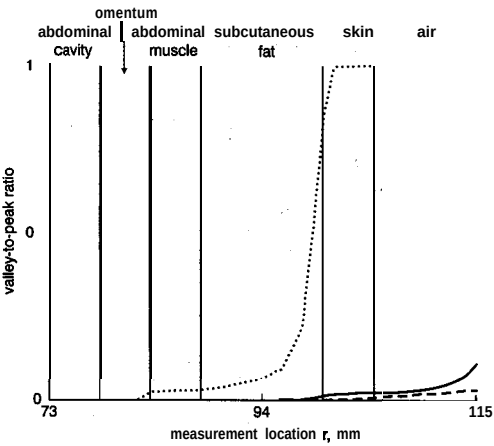

Fig. **13** *The valley-to-peak mtio of EENG and MENG source reconstructions increases at more superficial measurement locations. Sources reconstructed from EENG outside the subcutaneous fat layer do not meet the Rayleigh criterion and are considered unresolved. whereas MENG source reconstructions are all adequately resolved. (——) radial MENG; (- – -) tangential MENG; (· ·) EENG.*

Fig. 13 shows the imaging resolution of the source reconstructions in terms of the valley-to-peak ratios. Once again, the effect of the omentum and subcutaneous fat layer on the EENG is quite pronounced. EENG source reconstructions from the skin layer fail to meet the Rayleigh criterion and are considered unresolved. Both radial and tangential MENG source reconstructions are adequately resolved in all measurement locations.

4 Discussion

'This work introduces the first mathematical model for the magnetic fields from intestinal activity. Other authors have developed model simulations for the electrogastrogram and for gastric and intestinal electrical activity (DIAMANT *et al.,* 1970; MIRIZZI, **1985, 1986; KOTHAPALLI, 1993; FAMILONI** *et al.,* **1995; MINTCHEV and BOWES, 1995). Our** purpose in this work was to compare the electric potentials and the magnetic fields that result from intestinal electrical activity.

Our results show how the EENG and the radial and tangential MENG are attenuated and smoothed by abdominal layers. Measurements made more distant from the source reduce both the amplitude and spatial information in all signals. However, the presence of the low-conductivity layers of omentum and subcutaneous fat introduces additional adverse effects on the spatial properties of the EENG, reducing both its localising and imaging resolving power. We found that two sources separated by 5 cm were adequately resolved from inverse solutions from external MENG signals, but were not adequately resolved by cutaneous EENG inverse reconstructions. The spatial detail in the EENG signal is obscured since its forward spatial filters drop off rapidly at higher spatial frequencies. The rapid dropoff with spatial frequency implies that inverse filters must be severely regularised to avoid instability in the source reconstructions, and the regularisation process reduces the spatial resolution.

These results suggest that while the geometry of the abdominal volume conductor affects both signals equally, the conductivity profile has a greater effect on the EENG. To verify this notion, we calculated the maximum window cutoff frequency allowed for stable solutions (i.e., spatial resolution) while varying the conductivity and geometrical parameters of the models, as seen in Fig. 14. Except for the conductivity of the abdominal cavity, the MENG source reconstructions show no noticeable response to variations in the conductivity parameters. Low values of the abdominal cavity conductivity affect the membrane potential and so change the MENG source reconstructions, since the assumption that led to eqn 1 is no longer valid. On the other hand, EENG source reconstructions exhibit maxima in the spatial resolution (maximum window cutoff frequency) when the conductivity of adjacent layers approaches the same value. Thus, the *difference* in conductivity between two layers combined with the thickness of the layer affects the spatial resolution of EENG signals but exhibits no appreciable effect on the MENG. Furthermore, in actual practice, the abdominal layers simulated in this work may not be in physical contact which would further decrease the conductivity and thus, the quality of the EENG signal whereas the magnetic signal, mediated by tissue permeabilities, would not be as affected. We observe similar effects on both EENG and MENG signals from variations in geometrical parameters. These results are consistent with head model results that show that geometrical effects are much more pronounced than conductivity effects on magnetic fields (HAMALAINEN and **SARVAS,** 1989);

These results of our model simulations may explain why the magnetic fields of intestinal activity are able to be consistently recorded in every volunteer (**RICHARDS** *et al.,* 1996), while electric potentials of intestinal activity have proven quite difficult for cutaneous detection (**CHEN *et al.*, 1993*a*).** The

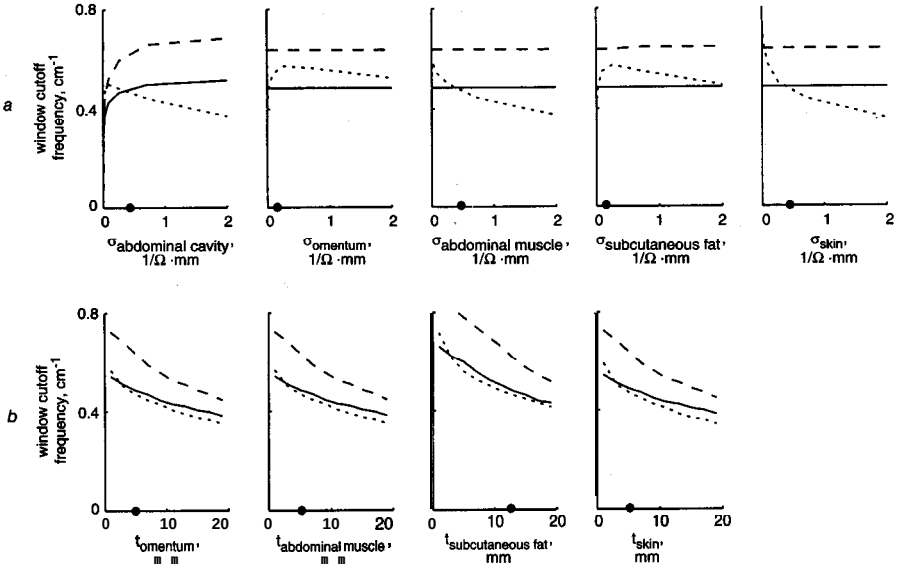

Fig. 14 *(a) When the conductivity pammeters are changed, little effect is seen on the spatial resolution of MENG source reconstructions (except for low values of the conductivity of the abdominal cavity, which affects the intestinal sources), while the EENG source reconstructions have greater resolution as the conductivities of adjacent layers approach the same value. (b) Geometrical parameter variations affect both EENG and MENG in similar manners. (——) radial MENG; (- – -) tangential MENG; (· ·) EENG; (•) nominal value.*

alternating low- and high-conductivity abdominal layers severely smooth the spatial information in the EENG signal as well as attenuate its amplitude.

In contrast, magnetic fields are not affected by conductivity properties of the volume conductor and thus, degrade primarily in response to geometrical considerations. For this reason, it is crucial that both EENG and MENG signals be measured as close as possible to the source. Furthermore, the tangential MENG is a stronger signal and retains more of its spatial properties throughout the model layers. Most current biomagnetometer systems record only the radial component of the magnetic field. The tangential magnetic field may provide higher quality information about internal sources of GI electrical activity.

These simulations assumed a small intestinal source, but the spatial filter approach could also be extended to signals from the stomach. The cutaneous EGG may not suffer from the same attenuation and smoothing seen in the cutaneous EENG since the signal strength may be stronger and there may be fewer conductivity discontinuities with thinner layers between the source and measurement locations. In fact, the postprandial EENG is significantly easier to record than the preprandial since distension of the stomach creates better contact witb the abdominal wall (MINTCHEV et al., 1993; CHEN and MCCALLUM, 1994).

Ultimately, the clinical utility of magnetic or electric detection of gastrointestinal electrical activity will lie in its ability to non-invasively identify gastric or intestinal abnormalities. Mesenteric ischemia, a condition in which the blood flow to a segment of the intestine is occluded, has been shown to reduce the temporal frequency of intestinal electrical activity in magnetic and electric recordings (RICHARDS et al., 1995). Because the magnetic fields from intestinal activity contain greater spatial detail than the electric potentials, it may be that such diseases can be diagnosed only with magnetic methods, since sufficient spatial resolution is required to separate ischemic from non-ischemic small bowel, and to separate bowel signals from other interfering signals. Likewise, diseases tbat affect the coupling of the gastric musculature may demand a method that allows clinicians to quantitatively delineate diseased regions of the stomach from healthy ones. Further study is needed to more fully elucidate source and volume conductor models under these conditions, and to evaluate the relative merits of electric and magnetic detection methods. The spatial filter analysis presented here provides a framework upon which such analyses can be based.

By framing the forward and inverse problems of the EENG and MENG in terms of spatial filters, we were able to visualize the effects of the abdominal layers on the spatial properties of the signals. Thus, fundamental considerations of the effects of these layers suggest that magnetic detection may avoid the dramatic decrease in the spatial properties of gastrointestinal electrical activity recorded by cutaneous electrodes.

Acknowledgments-This work was supported in part by grants from the National Institutes of Health (1 F32 DK09408-01) and the Department of Veterans Affairs. The authors wish to thank the reviewers for their insightful comments.

References

ABELL, T. L., CAMILLERI, M., and MALAGELADA, J.-R. (1985): 'High prevalence of gastric electrical dysrhythmias in diabetic gastroparesis', *Gastro*, 88, pp. 1299

ABELL, T. L., and MALAGELADA, J.-R. (1985): 'Glucagon-evoked gastric dysrhythmias in humans shown by an improved electrogastrographic technique', Gastro, 88, pp. 1932-1940

BEDI, B. S., KELLY, K. A., and HOLLEY, K. E. (1972): 'Pathways of propagation of the canine gastric pacesetter potential', *Gastro*, 63, pp. 288-296

BORN. M.. and WOLF. E. (1975): 'Principles of optics'. Pergamon Press, New York .

BRADSHAW, L. A. (1995): 'Measurement and Modeling of Gastrointestinal Bioelectric and Biomagnetic Fields'. PhD Dissertation, Vanderbilt University

BRADSHAW, L. A., ALLOS, S. H., WIKSWO, J. P., Jr., and RICHARDS, W. 0. (1997): 'Correlation and comparison of magnetic and electric detection of small *intestinal* electrical *activity', Am. J Phyiol., 272,* (Gastrointest. Liver Physiol. 35), pp. G1159-Gll67

BRADSHAW, L. A., LADIPO, J. K., STATON, D. J., WIKSWO, J. P., Jr., and RICHARDS, W. 0. (1999a): 'The human vector magnetogastrogram and magnetoenterogram', *IEEE Trans. Biomed. Eng., 46,* pp. 959-970

BRADSHAW, L. A., WIJESINGHE, R. S., and WIKSWO, J. P., Jr. (1996): 'A spatial filter model for analysis of the forward and inverse

problems of electroencephalography and magnetoencephalography', *Ann. Biomed. Eng. (in* press)
CHEN, J. D. Z., and MCCALLUM, R. W. (1994): 'Electrogastrogmphic parameters and their clinical significance', in CHEN, J. D. Z., and MCCALLUM, R. W. (Eds): 'Electrogastrography: principles and applications' (Raven Press, New York), pp. 45-73
CHEN, J., and MCCALLUM, R. W. (1992): 'Gastric slow wave abnormalities in patients with gastroparesis', *Am. J. Gastro.*, *87,* pp. 477-482
CHEN, J. D. Z., SCHIRMER, B. D., and MCCALLUM, R. W. (1993*a*): 'Measurement of electrical activity of the human small intestine using surface electrodes', *IEEE Trans. Biomed. Eng.*, *40*, pp. 598–602
CHEN, J. D. Z., RICHARDS, R, and MCCALLUM, R. (19936): 'Frequency components of the electrogastrogram and their correlations with gastrointestinal motility', *Med. Biol. Eng. Comput.*, 31, pp. 60–67
DANIEL, E. E., D. R., WACHTER, B. T., SUTHERLAND, W. H., and BOGOCH, A. (1959): 'Electrical activity of the small intestine', *Gastro*, 37, pp. 268–281
DANIEL, E. E., and SARNA, S. (1978): 'The generation and conduction of activity *in* smooth muscle', *Ann. Rev Pharmacol. Toxicol.*, 18, pp. 145-166
DEBINSKI, H. S., AHMED, S., MILLA, P. J., and KAMM, M. A. (1996): 'Electrogastrography in chronic intestinal pseudoobstruction', Dig. *Dis. Sci.*, **41(7),** pp. 1292-1297
DEVANE, S. I!, RAVELLI, A. M., BISSET, W. M., SMITH, V V, LAKE, B. D., and MILLA, I? J. (1992): 'Gastric antral dysrhythmias in children with chronic idiopathic intestinal pseudoobstruction', Gut, 33, pp. 1477-1481
DIAMANT, N. E., ROSE, P K., and DAVISON, E. J. (1970): 'Computer simulation of intestinal slow-wave frequency gradient', *Am. J. Physiol.*, 291, pp. 1684-1690
FAMILONI, B. O., BOWES, K. L., KINGMA, Y. J., and COTE, K. R. (1991): 'Can transcutaneous recordings detect gastric electrical abnormalities?', Gut, 32, pp. 141-146
FAMILONI, B. O., ABELL, T. L., and BOWES, K. L. (1995): 'A model of *gastric electrical* activity in health and disease', *IEEE Trans. Biomed. Eng.*, *42,* pp. 647-657
FLECKENSTEIN, I? (1978): 'Migrating electrical spike activity in the fasting human small intestine', *Amer. J. Dig. Dis.*, *23,* pp. 769-775
HAMALAINEN, M. S., and SARVAS, J. (1989): 'Realistic conductivity geometry model of the human head for interpretation of neuromagnetic fields', *IEEE Trans. Biomed. Eng.*, 36, pp. 165-171
HASLER, W. L., KIM, M. S., CHEY, W. D., STEVENSON, V., STEIN, B., and OWYANG, C. (1995): 'Central cholinergic and alpha-adrenergic mediation of gastric slow wave dysrhythmias evoked during motion sickness', *Am. J. Physiol.*, *268,* pp. G539–G547
HONGO, M., and OKUNO, Y. (1993): 'Diabetic gastropathy in patients with autonomic neuropathy', *Diab. Med.*, *10,* (Supp. 2), pp. 79S–81S
KOCH, K. L., STERN, R. M., STEWART, W. R., VASEY, M. W., and SULLIVAN, M. L. (1989): 'Gastric emptying and gastric myoelectric activity in patients with symptomatic diabetic gastroparesis: Effects of long-term domperidone treatment', Am. *J. Gastroenterol.*, 84, pp. 1069–1075
KOCH, K. L., STERN, R. M., VASEY, M., BOTTI, J. J., CREASY, G. W., and DWYER, A. (1990): 'Gastric dysrhythmias and nausea of pregnancy', *Dig. Dis. Sci., 35,* pp. 961-968
KOTHAPALLI, B. (1993): 'Electrogastrogram simulation using a three-dimensional model', *Med. Biol. Eng. Cornput.*, 31, pp. 482-486
MINTCHEV, M. P., and BOWES, K. L. (1995): 'Conoidal dipole model of electrical field produced by the human stomach', *Med. Biol. Eng. Comput.*, *33,* pp. 179-184
MINTCHEV, M. P., and BOWES, K. L. (1997): 'Do increased electrogastrographic frequencies always correspond to internal tachygastria?', *Annals of Biomed. Eng.*, *25,* pp. 1052-1058
MINTCHEV, M. P., KINGMA, Y. J., and BOWES, K. L. (1993): 'Accuracy of cutaneous recordings of gastric electrical activity', *Gastro*, 104, pp. 1273-1280
MINTCHEV, M. P., STICKEL, A., OTTO, S. L., and BOWES, K. L. (1997): 'Reliability of percent distribution of power of the electrogastrogram *in* recognizing *gastric electrical* uncoupling', *IEEE Trans. Biomed. Eng.*, 44, pp. 1288-1291
MIRIZZI, N., STELLA, R., and SCAFOGLIERI, U. (1985): 'A model of extracellular waveshapes of gastric electrical activity', Med. *Biol. Eng. Comput., 23,* pp. 33-37
MIRIZZI, N., STELLA, R., and SCAFOGLIERI, U. (1986): 'Model to simulate the gastric electrical control and response activity on the abdominal wall and on the abdominal surface', *Med. Biol. Eng. Comput.*, 24, pp. 157-163
PARKER, R. L. (1977): 'Understanding inverse theory', *Ann. Rev Earth Planet. Sci., 5,* pp. 3564
PFISTER, C. J., HAMILTON, J. W., NAGEL, N., BASS, P., WEBSTER, J. G., and TOMPKINS, W. J. (1988): 'Use of spectral analysis in the detection of frequency differences in the electrogastrograms of normal and diabetic subjects', *IEEE Trans. Biomed. Eng., 35,* pp. 935-941
RICHARDS, W. O., GARRARD, C. L., ALLOS, S. H., BRADSHAW, L. A., STATON, D. J., and WIKSWO, J. P., Jr. (1995): 'Noninvasive diagnosis of mesenteric ischemia using a SQUID magnetometer', *Ann. Surg.*, 221, pp. 696705
RICHARDS, W. O., BRADSHAW, L. A., STATON, D. J., GARRARD, C. L., LIU, F., BUCHANAN, S., and WIKSWO, J. I?, Jr. (1996): 'Magnetoenterography (MENG): Noninvasive measurement of bioelectric activity in human small bowel', *Dig. Dis. Sci.*, 41, pp. 2293-2301
ROTHSTEIN, R. D., ALAVI, A., and REYNOLDS, J. C. (1993): 'Electrogastrography in patients with gastroparesis and effect of long-term cisapride', *Dig. Dis.* Sci, 38, pp. 1518-1524
SMOUT, A. J. P M., VAN DER SCHEE, E. J., and GRASHUIS, J. L. (1980): 'What is measured in electrogastrography?', *Dig. Dis. Sci.*, 25, pp. 179187
SMOUT, A. J. P M., VAN DER SCHEE, E. J., AKKERMANS, L. M. A., and GRASHUIS, J. L. (1984): 'Recording of gastrointestinal electrical activity from surface electrodes'. *Scand. J. Gastroenterol.*, Suppl. 96, pp. 11-18
TELANDER, R. L., MORGAN, K. G., KREULAN, D. L., SCHMALZ, P. F., KELLY, K. A., and SZURSZEWSKI, J. H. (1978): 'Human gastric atony with tachygastria and gastric retention', *Gastro*, **75,** pp. 497-501
WOOSLEY, J. K., ROTH, B. J., and WIKSWO, J. P, Jr. (1985): 'The magnetic field of a single axon: A volume conductor model', *Math. Biosci., 76,* pp. l-36
You, C. H., LEE, K. Y., CHEY, W. Y., and MENGUY, R. (1980): 'Electrogastrographic study of patients with unexplained nausea, bloating, and vomiting', *Gastro*, 79, pp. 311-314

Authors' biographies

ALAN BRADSHAW received his BS in Physics from Abilene Christian University in 1990, and MS and PhD in 1992 and 1995 from Vanderbilt University. He continued his work in gastrointestinal biomagnetism under an NIH National Research Service Award from 19961998. He now serves as Director of the Biomagnetism Laboratory and is appointed as Research Assistant Professor in the Department of Physics at Vanderbilt University and in the Department of Surgery at Vanderbilt University Medical Center. He is also an Assistant Professor of Physics at Lipscomb University. His research interests include magnetic and electric detection of gastrointestinal activity and mathematical modelling of bioelectric activity.

WILLIAM 0. RICHARDS was born in Ann Arbor, Michigan in 1953. He received his MD from the University of Maryland, Baltimore in 1979. After finishing his residency in general surgery in 1984 he completed a Research Fellowship in GI Physiology at Vanderbilt University in 1987. He is currently a Professor of Surgery at Vanderbilt University School of Medicine. His current research interests include the electrophysiology of gastrointestinal smooth muscle.

JOHN P. WIKSWO received his BA in Physics from the University of Virginia and his MS and PhD in Physics from Stanford University. He was a Research Fellow in Cardiology at the Stanford University School of Medicine from 1975 to 1977. He joined the faculty in the Department of Physics and Astronomy at Vanderbilt University as an Assistant Professor of Physics in 1977. He is now a Professor of Physics and the A.B. Learned Professor of Living State Physics. He has been a Woodrow Wilson Fellow, an NSF Predoctoral Fellow, an Alfred P. Sloan Research Fellow, and a John Simon Guggenheim Fellow, and is a fellow of the American Physical Society. At Vanderbilt, his research has been directed primarily towards using novel instrumentation. electric and magnetic measurements. and electromagnetic theory for studying the propagation of electrical activity in isolated and in vivo nerves, skeletal muscle and cardiac muscle, and for non-destructive testing.